Environ Earth Sci (2016) 75:1231
DOI 10.1007/s12665-016-6011-9

THEMATIC ISSUE

Kinetics of dissolution processes in loess-like sediments and carbonate concretions in the southeast of the province of Buenos Aires, Argentina

M. Vital[1] · D. E. Martínez[1] · N. Borrelli[1] · S. Quiroga[2]

Received: 25 May 2015 / Accepted: 16 May 2016 / Published online: 7 September 2016

Abstract The Pampeano aquifer formed by loess-like sediments provides water to cities and for agricultural uses in the Pampean plain, which is the most productive area in Argentina. Studies on the mechanisms through which this groundwater acquires its chemical composition are scarce and generally make assumption about equilibrium conditions. Few works on total sediments kinetics of mineral dissolution have been made. The main objective is to characterize ions incorporation to the groundwater of the Pampeano aquifer and to estimate the rate of the dissolution of the solid phase of the Pampeano sediments. This work also aims to provide evidence on the effect of particles size on water chemistry, and the changes in mineral structure during dissolution. The methodology included batch experiments on loess and calcrete during 10 h. The kinetics of ions incorporation into water presented variations depending on the types of sediments dissolving and the sizes of particles. Steady values were reached in the first minutes of reaction. Although the principal components of the Pampeano aquifer like calcite, quartz and aluminosilicates are known to have low dissolution coefficient, ions were incorporated fastly into water and saturation of solution appeared in the first minutes of the experiments. Saturation index (SI) calculated by PHREEQC also showed sensitivity to particles size. Observations with loupe and microscope showed modifications on the sediments appearance after batch reactions. For instance, porosity in calcrete increased. Increments in BET (Brunauer–Emmett–Teller) surface area and micropore surface area were measured. Significant changes in sediment chemistry measured by SEM/EDS were observed as well during dissolution processes.

Keywords Kinetics of dissolution · Loess-like sediments · Calcrete concretions · Batch experiments

Introduction

The Pampeano sediments in Argentina cover an area of 1,800,000 km^2 (Ameghino 1880). The term "Pampeano sediments" is an informal term and considers the eolian Quaternary deposits of the Pampean region. They are mostly constituted by silt, which is more abundant than the subordinated sand and clay fractions. Those sediments are considered as a loess formation, but their composition in Argentina is different from typical loess because of the high content of volcanic glass and feldspars (Tricart 1973; Pye 1995). Another important component of this formation is calcrete, which forms on calcareous materials ($CaCO_3$). The mineralogical composition of the Pampeano aquifer is homogeneous, and most of its components come from volcanic eruptions (Teruggi 1957; Tricart 1973). Its thickness ranges between 30 and 100 m (Auge and Hernández 1984).

These deposits have a primary porosity that gives an aquifer behavior from a hydrogeological point of view. The Pampeano aquifer is very important because it contributes

This article is part of a Topical Collection in Environmental Earth Sciences on ''3RAGSU'', guest edited by Daniel Emilio Martinez.

✉ M. Vital
ingagr.melanie.vital@gmail.com

[1] Instituto de Geología de Costas y Cuaternario (UNMP - CIC) - Instituto de Investigacion Marina y Costera (CONICET - UNMDP), 7600 Mar Del Plata, Buenos Aires, Argentina

[2] Departamento de Química, Facultad de Ciencias Exactas, Universidad Nacional de Mar del Plata, Buenos Aires, Argentina

to 60 % of the Argentinian Gross Domestic Product (Schultz and Castro 2003) and provides water to cities and agriculture in the whole province of Buenos Aires. Nevertheless, there is relatively scarce research on how the water acquires its composition in this region. Many studies provide evidence on the susceptibility of the Pampeano aquifer to pollution. This includes for instance organic contamination (Martinez et al. 2004; Herrero and Fernández 2008), high salt content in some areas due to water intrusion (Bocanegra 1993; Bocanegra et al. 1995, 2002; Martinez et al. 1995) or high concentrations of fluoride and arsenic (Kruse and Ainchil 2003; Paoloni et al. 2003; Gomez and Martinez 2010; Martinez and Osterrieth 2013). All these studies, including those using numerical modeling as a tool for understanding geochemical processes, assume equilibrium conditions between the water and the solid matrix of the aquifer. Although the natural water chemistry is controlled by both thermodynamic principles of chemical equilibrium and kinetic (Fagundo et al. 2004), it is mostly studied from the viewpoint of chemical equilibrium (Garrels and Christ 1965). In this case, the role of the time factor in the processes of mineral weathering is not considered (Fagundo et al. 1996). One of the most important geochemical processes in an aquifer is mineral dissolution, as it greatly affects the quality of potable water (Brantley et al. 2008).

The mean residence time (MRT) of the young water component of the Pampeano aquifer in the study area ranges around 20–40 years (Martinez et al. 2015), and as groundwater is moving, there can be reactions not reaching equilibrium during mineral dissolution. For example, in this aquifer, most of the mineral components are silicates, minerals of low solubility. To improve the quality of numerical tools used to study the chemical composition of the groundwater in this area, it is important to take into account the kinetics of reactions.

Most common kinetics studies are developed to determine the dissolution rates of monominerals. The kinetics rates of quartz dissolution were measured in various conditions of temperature (Brady and Walther 1990; Tester et al. 1994), water chemical composition (Dove and Crerar 1990; Dove 1999) and pH (House and Orr 1992; Xiao and Lasaga 1996). Similar experiments were completed on various types of silicates (Luce et al. 1972; Brady and Walther 1989; White and Brantley 1995; Cama et al. 2000; Dixit and Carroll 2007; Daval et al. 2013) and carbonates (Morse 1983; Chou et al. 1989; Pokrovsky and Schott 2002). The high variability of chemical composition in total sediments explains the common use of purified minerals (Morse 1978; Van Cappellen 1996; Van Cappellen and Qiu 1997), in studies of kinetics of dissolution. To determine dissolution kinetics, batch reaction experiments (Brantley et al. 2008) or flow-through experiments (Critelli et al. 2014, 2015) can be used. Rates law can be calculated from the amounts of a chemical element released in solutions over time. Vertical scanning interferometry, a more recent technique, enables calculating more accurately rate dissolution laws by measuring the change of surface height with time (Lüttge 2005; Smith et al. 2013; Daval et al. 2013).

This work is a first step in the description of the mechanisms in which water acquires its composition when it is in contact with Pampeano sediments. Batch reaction was used to evidence the main chemical processes during dissolution of loess and calcrete. Representative samples of the Pampeano sediments were selected to perform batch reaction of dissolution in function of grain size, to determine ions incorporation rates in solution. Modifications in aspect, structure and chemistry were observed to evaluate the consequences of the dissolution process on minerals.

Materials and methods

Samples recollection

Samples of calcrete (C1), loess sediments (L1), and a sample of calcrete on the limit contact layer with loess (M1) that is mostly impure calcrete, were gathered from an outcrop in the area of Mar del Plata (Fig. 1) in the province of Buenos Aires, Argentina (−38.086860, −57.649185). This area was chosen because it is representative of the mineral composition of the Pampeano aquifer in this sector of the Pampa plain, and because the outcrop is including both loess-like and calcrete sediments (Fig. 2).

Samples preparation

In order to compare the effect of particle size on ions incorporations rates, experiments were realized on total sediments (L1, C1) and sieved sediments (L2, C2, M2). To obtain the sieved sample, total samples were sieved and only the fraction corresponding to grain size under PHI 3 or 0.088 mm was used. This corresponds to fractions of very fine sand, silt and clay in the case of loess. Then, all samples were dried in a culture incubator FANEM at a temperature of 50 °C for 48 h.

Dissolution experiments

The methodology consisted of batch type tests lasting 10 h on 2.5 g of each sample. Essays were performed in Falcon tubes in an orbital shaker TS-1000 at 200 rpm at ambient

Fig. 1 Location of the sample area (*red circle*)

temperature (25 °C). Samples previously dried were introduced in the falcon tubes, filled up to 50 ml with ultrapure water and agitated during 1, 5, 10, 15, 30, 45, 60, 90, 120, 180, 240, 300 and 1020 min. For each shaking time, three tubes were prepared. Once completed the stirring time, the falcon tubes were centrifuged in Colcor brand equipment for a period of 2 min at 750 rpm and filtered with Millipore filters of 0.45 microns pore size. The water solution was stored in plastic bottles, and the pellets were kept apart and dried at a temperature of 50 °C for 48 h.

For each stirring time, measurements of conductivity, temperature, alkalinity and pH on water samples were conducted. Temperature and conductivity were measured with WTW Cond 197i equipment. The pH was determined with pH meter N6123. Water potentiometric titration allowed to estimate alkalinity (mg/L of HCO_3^-) in water. Flame photometry was used to determine Ca^{2+}, Na^+ and K^+ concentration. Fluoride concentrations were obtained using direct colorimetry with Alizarin and silica content by UV–Vis spectrophotometry with the silicomolybdate method.

Data processing

Experimental data were analyzed with the program Origin 7. A first-order reaction process equation was adjusted to the experimental results. This enabled to calculate the values of k and $[A]0$. The rate constant is represented by k, and $[A]0$ is the concentration of ions in solution at infinite time. The initial rate of ion incorporation in solution was then calculated with Eq. (1).

$$r = k[A]0 \quad (1)$$

Saturation index was calculated for some minerals with the code PHREEQC (Parkhurst and Appelo 1999). The code NETPATH (Plummer et al. 1991) was used to check the mass balance of the proposed processes.

Analyses on sediments

The distribution of L1 particle sizes was determined with sieve analysis (Ingram 1971) using the Folk and Ward method (1957). In order to determine the mineralogical

Fig. 2 Picture of the Pampeano aquifer where samples of calcrete C1 *A*, mixed sample of calcrete and loess M1 *B*, and loess L1 *C* have been collected

composition of the sediments, 30 g of L1 and C1 was sent to INMAT laboratory, UNICEN University, Province of Buenos Aires, Argentina. Samples were analyzed by X-ray diffraction with Philips Analytical X-Ray B.V. PC-APD diffraction software.

The pellets of L1 and C1 were analyzed by binocular loupe (×20) and a Petrography Microscope Olympus Bx51TF (×400) before and after 1020 min of reaction. The pellets of C2, L2 and M2 were separated to observe the changes in the smallest sediment grains structure and chemical composition. The Brunauer–Emmett–Teller (BET) methodology (Fagerlund 1973) and Micropore surface area measurements were performed on L2 and C2 before and after batch reactions in the CINDECA laboratory, La Plata, Buenos Aires. Semi-quantitative analyses on L2, C2 and M2 before and at the end of experiments were performed with a scanning electron microscope (SEM) and EDAX technology (SEM/EDS), at the microscopy laboratory from the National University of Mar del Plata. Each sample was measured 15 times to obtain a general average of its chemical composition in percentage of its weight (%w). To compare the semi-quantitative composition of the samples before and after the essays, Wilcoxon signed-rank test for paired data was applied to the chemical elements, since normality and homoscedasticity assumptions were not achieved (Zar 1984).

Results

Physical properties and mineralogical characterization

According to the particle size distribution (PSD) determination, L1 is constituted by 23 % of medium sand, 15 % of fine sand, 25 of very fine sand and 37 % of pelites (silt and clay). X-ray crystallography showed that minerals composing loess are quartz (SiO_2), albite ($NaAlSi_3O_8$), anorthite ($CaAl_2Si_2O_8$), brucite ($Mg(OH)_2$) and anatase (TiO_2). The calcrete mineral composition is calcite ($CaCO_3$), quartz, albite and anorthite. Amorphous minerals cannot be identified by the used analytical method.

Dissolution experiments

Water analysis

Discontinuous reactions of dissolution were performed on loess and calcrete. These experiments allowed observing the changes in water chemistry after dissolving processes and the influence of grain size (Figs. 3, 4, 5, 6, 7 and 8). First-order reaction laws have been used to fit curves to experimental data. In most experiments, steady values of ions concentration were reached between the first minute and 400 min of reaction.

The pH and ion concentration in these experiments are in general steady between 1 and 400 min of reaction, except for bicarbonates in calcrete C1 and C2 and silica in loess L2 where concentration keeps on increasing during all batch reaction. pH evolution is shown in Fig. 3. L2 and C2 samples present a higher pH of almost 1 unit. The highest pH of 8.5 can be obtained when C2 is reacting.

Bicarbonate concentration when sieved calcrete reacts does not get stable and reaches 12 mmol/L. It is twice the concentration obtained with C1 or M2. Bicarbonate content of water with L1 and L2 is similar and much lower of approx. 0.65 mmol/L (Fig. 3b).

Water calcium content is almost ten times higher when samples of loess dissolve. It is stable around 3 mmol/L in loess, whereas this value is steady at approx. 0.3 mmol/L for calcrete (Fig. 4a). In addition, calcium concentration is more important when samples are not sieved for both loess and calcrete.

More sodium is released when loess is not sieved and sodium concentration in loess is almost twice the concentration obtained with calcrete (Fig. 4b). On the contrary,

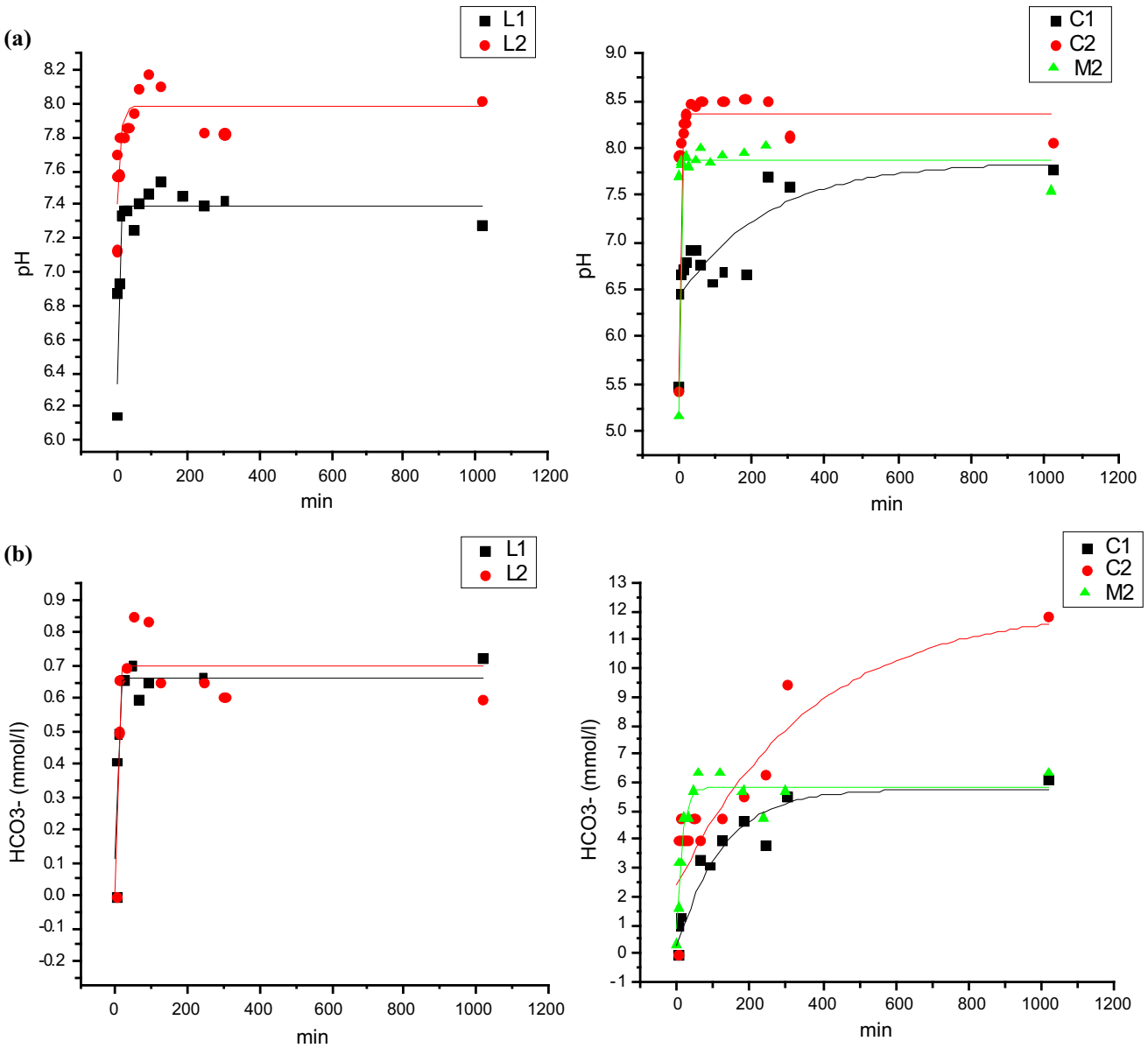

Fig. 3 Kinetics of water pH (**a**) and incorporation of HCO_3^- (**b**) into water during batch reaction of dissolution of loess and calcrete

there is more sodium when calcrete is sieved. Sample M2 shows an intermediary concentration of 1.7 mmol/L.

Dissolved silica content in water reacting to M2 increases until 2.97 mmol/L (Fig. 5a). This concentration is twice the concentration obtained when sieved calcrete is reacting. Content of silica in water dissolving loess is much lower, under 1 mmol/L, and sieved loess (L2) does not reach a steady value.

The dissolution of sample C2 results in a much higher sulfates concentration than other experiments and stabilizes around 2.39 mmol/L. Water sulfates concentration with L1, L2 and C1 is steady around 0.3 mmol/L (Fig. 5b). Potassium release in water in both loess and calcrete is slightly higher when sieved sediments are used. M2 and L2 present the greatest potassium content of approx. 0.17 and 0.18 mmol/L (Fig. 6a). With calcrete sample C2, the higher concentration of fluoride of 0.12 mmol/L is reached. On the contrary, more fluoride is found in solution when loess is not sieved (Fig. 6b).

The rate r of incorporation of each element in mmol/min in water during batch experiments was calculated with Eq. (1) from the value of the parameters A[0] and k determined by Originlab7 (Table 1). In some cases, experimental data could not be adjusted to the simulated fitting curves, particularly for calcium in L1, C1 and M2 and sodium in C1 and M2. These results are caused by

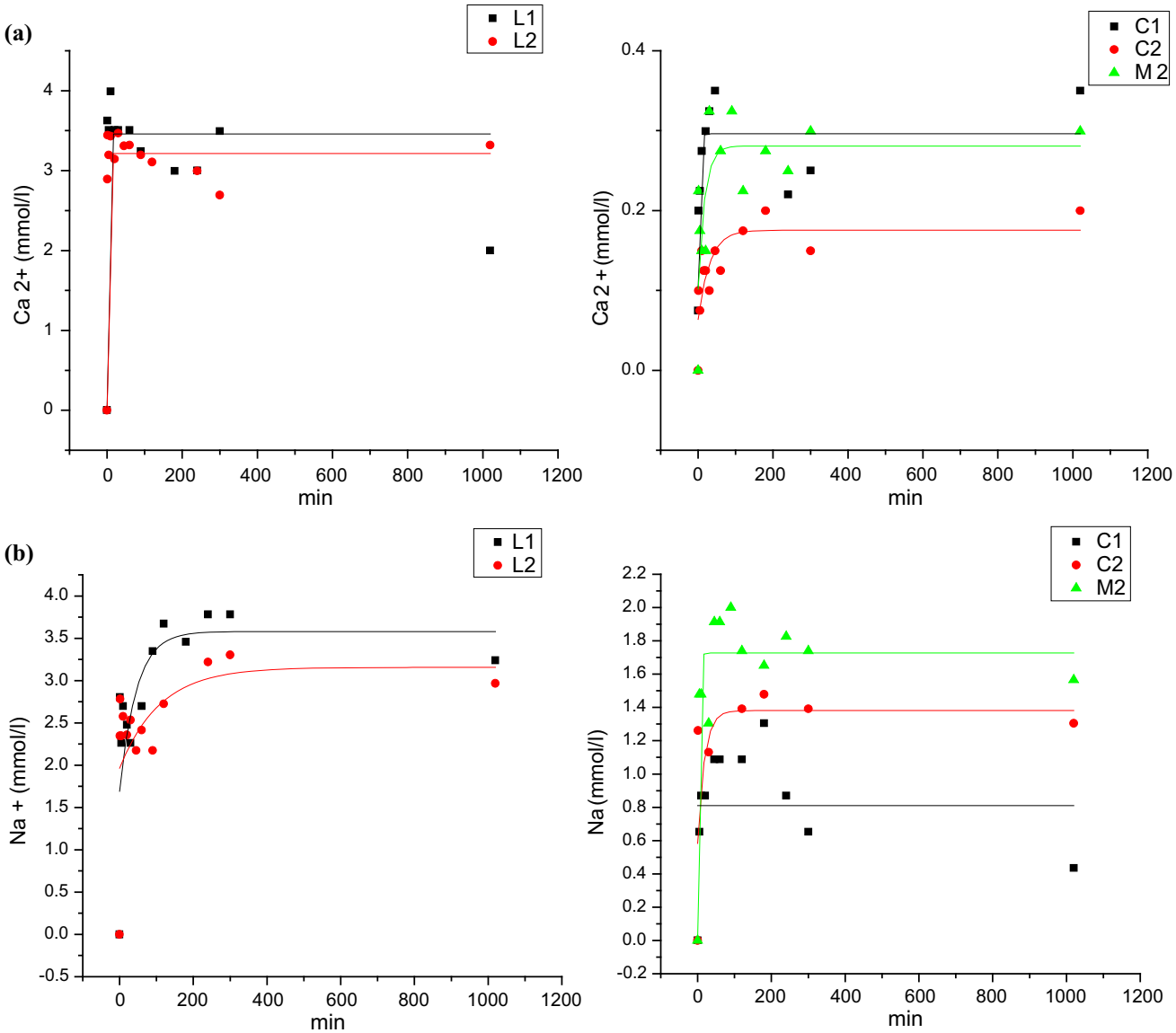

Fig. 4 Kinetics of incorporation of Ca^{+2} (**a**) and Na^{+} (**b**) into water during batch reaction of dissolution of loess and calcrete

variations of the flame photometer during measurements. The rates were not calculated in those last cases. The highest incorporation rate is observed for calcium in dissolution of L2 with 0.787 mmol/min followed by bicarbonate in dissolution of M2 with 0.439 mmol/min. Sieved calcrete C2 presents the lowest rate of calcium incorporation with only 0.006 mmol/L. In Table 1, the final concentration in solutions A[0] for each sample can be related to a groundwater sample from a reference study of Martinez et al. (Martinez and Osterrieth 2013). Compared to this groundwater sample, C1, C2 and M2 have the closest concentration of bicarbonate, between 5.7 and 12.3 mmol/L compared to 9.46 mmol/L. However, L1 and L2 show the most similar concentration in calcium and sodium. L2 is closer for SiO_2 content (0.7 mmol/L), and M2 has almost three times more silica (2.97 mmol/L) than the reference groundwater sample (0.98). The sulfates content is closer when C2 dissolves with 0.184 mmol/L.

Saturation index of calcite, quartz and amorphous silica was calculated for each experiment with the program Phreeqc (Parkhurst and Appelo 1999). For L1, the values of saturation index of calcite and silica are under 0 during all reaction (Fig. 5a), while it reaches almost 0.8 for quartz. In dissolution of L2, SI of calcite and quartz goes over 0 in the first minutes of reaction. SI of silica stays under 0 in this experiment (Fig. 6b). When C1 is reacting SI of calcite is negative during almost all the reaction time, but then it is positive at time 1020 min (Fig. 5c). During batch experiment with C2, SI of calcite is approx. −0.5, and then, after 25 min of dissolution, it fluctuates around 0.3. SI of silica

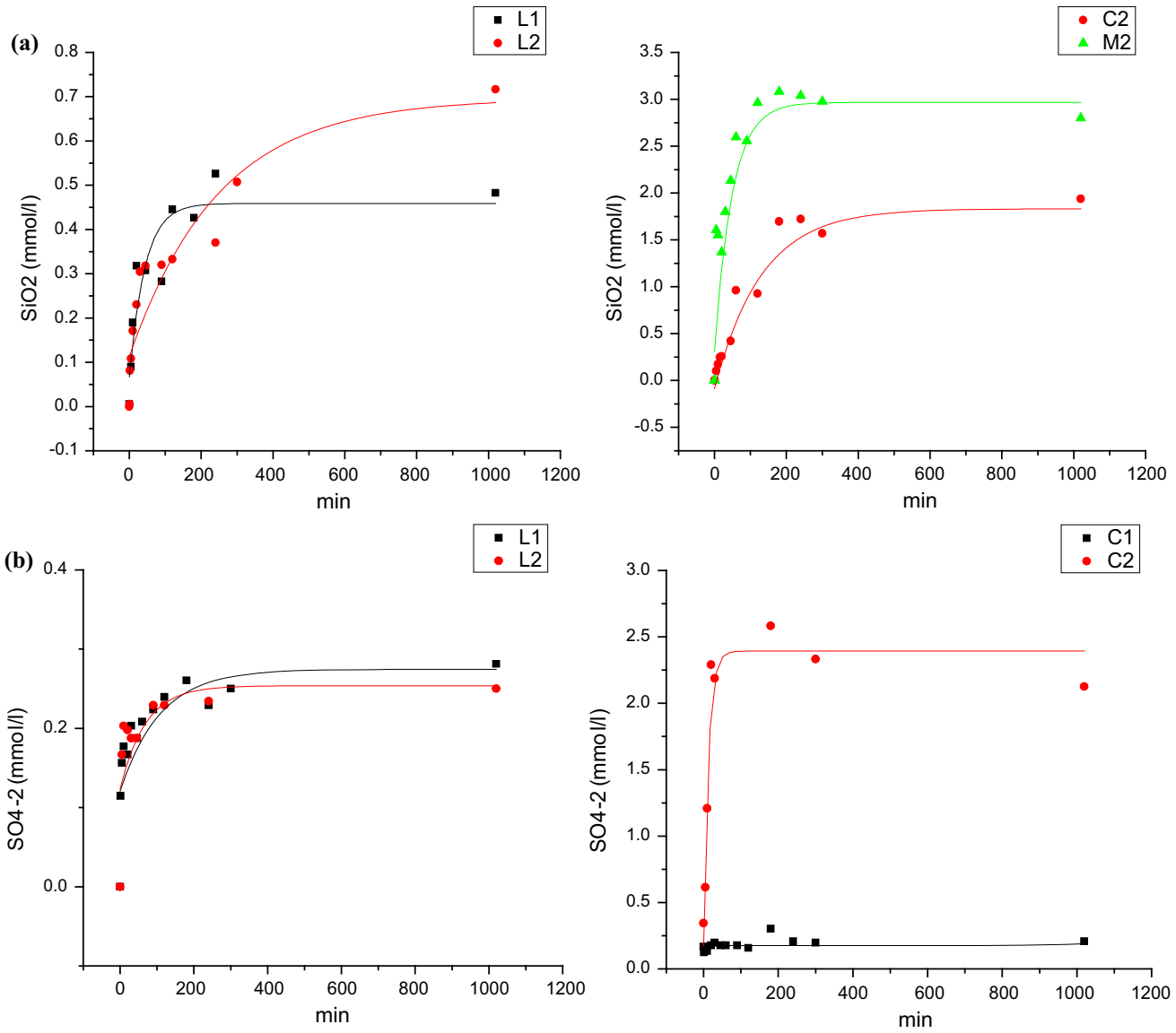

Fig. 5 Kinetics of incorporation of SiO_2 (**a**) and $SO4^{-2}$ (**b**) into water during batch reaction of dissolution of loess and calcrete

goes above 0 after 1020 min of reaction (Fig. 5d). Finally, SI of calcite was calculated when batch reactions is made with M2 (Fig. 5e). After 50 min, SI reaches 0.1 and is again under 0 at time T1020. SI of silica in that experiment varies around 0.1 after 50 min and is steady until the end of the experiment. For C1, C2 and M2, SI of quartz reaches values of 1.2–1.5 in 200 min of reaction.

Inverse models obtained by using NETPATH and considering pure water as initial solution and L2, C2, M2 as finals solutions for three different models showed that calcite dissolution involves CO_2 incorporation, cation exchange, releasing sodium and uptaking calcium, and gypsum dissolution (Table 2). It is also possible to observe that calcrete (C2) and impure calcrete (M2) reactions involve the dissolution of double calcite amounts than for loess samples (L2) and the Ca^{2+} release to water promote a higher cationic exchange process. Gypsum dissolution is needed in order to explain sulfur increase after L2 and C2 reactions, but not significant when M2 reacts.

Sediments analysis

The observation of loess sediments before batch reaction with binocular loupe (×20) shows presence of aggregates and isolated minerals. After contact with water, the smallest aggregates and mineral cannot be observed anymore. With the microscope, only the thickest aggregates can be seen (Fig. 6a). Calcrete before dissolution is observed as a clean mineral with a plain surface, which is one of the characteristics of this mineral. After reacting

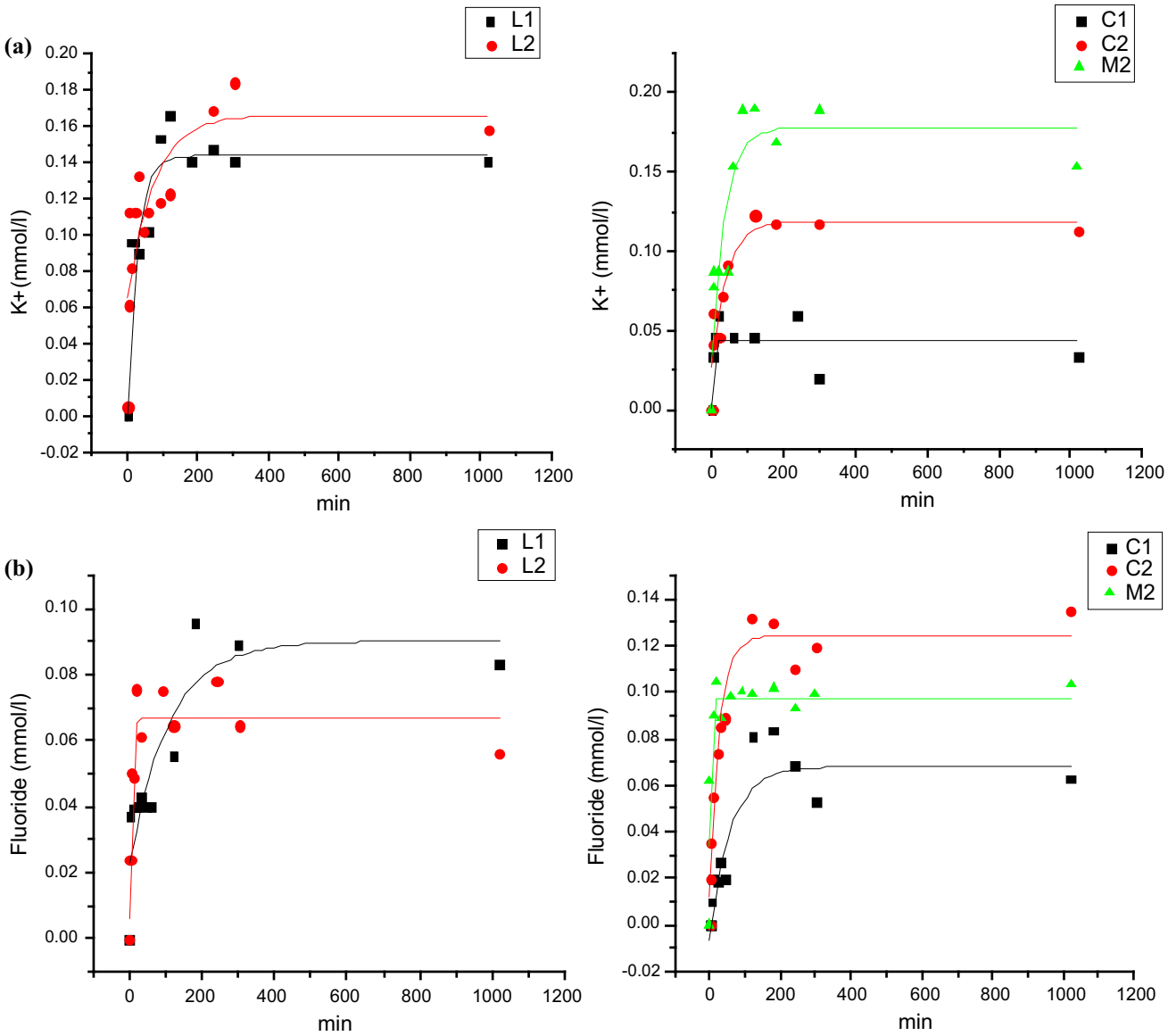

Fig. 6 Kinetics of incorporation of K^+ (**a**) and F^- (**b**) into water during batch reaction of dissolution of loess and calcrete

with water, the surfaces have a high level of porosity. At the microscope, small particles of calcium carbonates were observed before dissolution, while after contact with water, the smallest particles of calcium carbonate have mostly disappeared (Fig. 6b).

Loess samples (L2) have a greater surface area from BET determinations, 56.6302 ± 0.8004 m^2/g, than the calcrete (C2), 41.7315 ± 0.1128 m^2/g. After 1020 min of contact with water, the surface area increases in both materials to 57.9663 ± 0.3366 m^2/g (L2) and 43.1886 ± 0.1206 m^2/g (C2). The same trend was observed in relation with the micropore area, increasing after dissolution from 8.1529 to 11.6073 m^2/g in L2; and from 9.5865 to 11.5713 m^2/g in C2.

SEM and EDAX analysis of loess (L2) before contact with water shows that it is mainly composed of silicon, 38–60 %, aluminum, 12–30 % and carbon, from 5–20 % (Table 3). Those proportions remain stable after the dissolution, except for the carbon that is almost 5 % lower after batch reaction (T: −79, p: 0.0137). Sodium, magnesium, chlorides, potassium, calcium, titanium and manganese compose all together less than 15 % of the loess sample. Most of the percentages of those elements are similar after dissolution except for manganese (T: 105, p: 0.001), magnesium (T: 99, p: 0.0019) and titanium (T: 96, p: 0.0027) that tend to disappear or decrease, instead potassium (T: −105, p: 0.001) and calcium (T: −105, p: 0.001) that tend to increase. Iron proportions are slightly

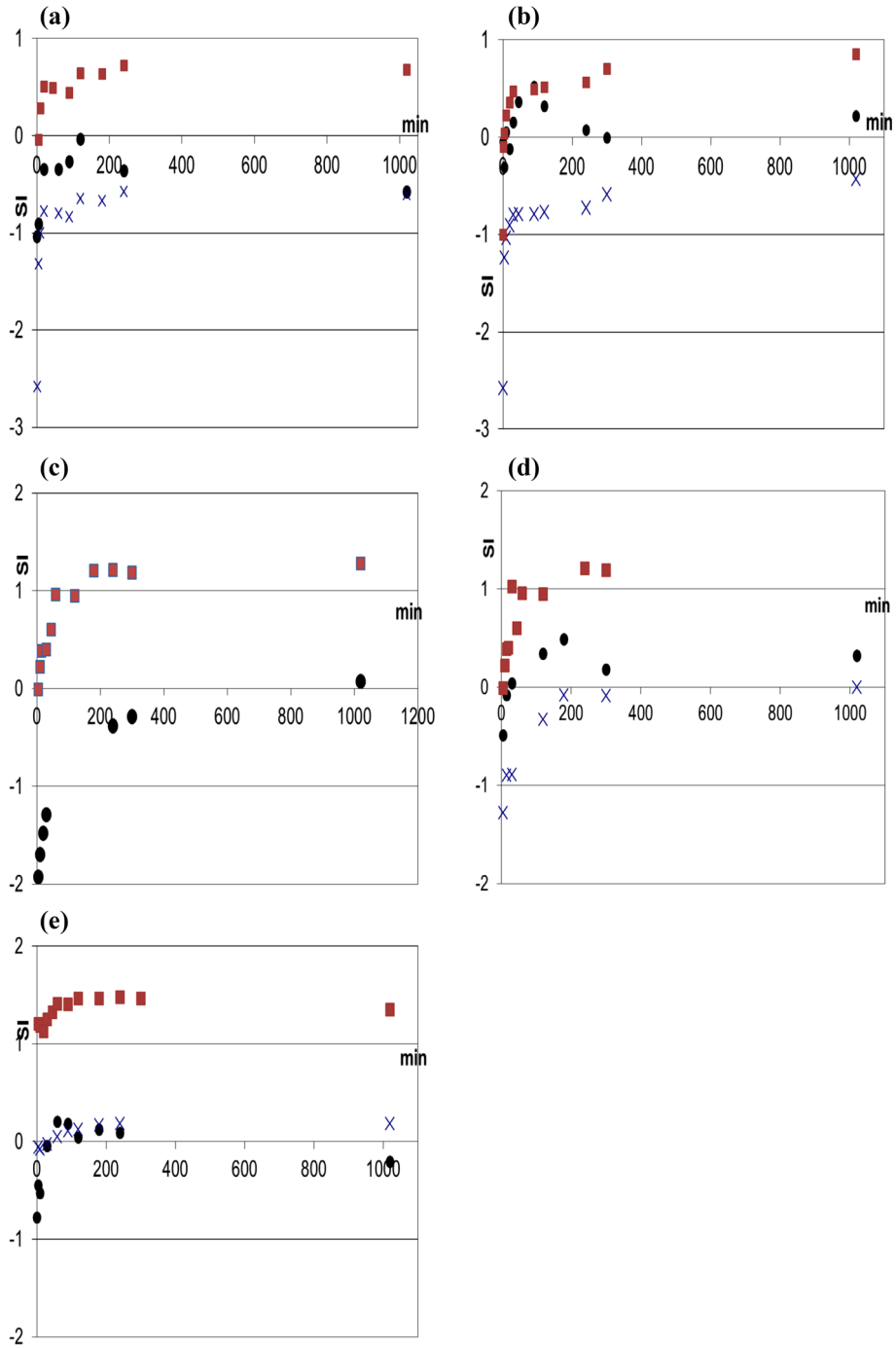

Fig. 7 Saturation index kinetics of calcite (*black circle*), quartz (*black square*) and silica (*x*) for loess L1 (**a**), L2 (**b**) and calcrete C1 (**c**), C2 (**d**), M2 (**e**) in batch experiments of dissolution

higher after dissolution and go from less than 1 % before contact with water to values around 8 % (T: −105, p: 0.001, Table 1).

In C2, the main components before dissolution are carbon, 29–43 %, calcium, 20–40 %, and silicon, 0–19 %, followed by aluminum, around 8 %. After dissolution, the carbon content is 10 % higher (T: −120, p: 0.0007), while the silicon content decreases about 5 % (T: 101, p: 0.004, Table 1). Sodium, magnesium, chlorides, potassium and iron represent less than 10 % and decrease their content or disappear after dissolution (T(Mg): −101, p: 0.004; T(Cl): 117, p: 0.0009; T(K): 90, p: 0.01; T(Fe): 92, p: 0.009). The analysis of M2 shows that the major components of this sediment are carbon, 18–41 %, silicon, 22–34 %, calcium, 17–26 % and aluminum, 6–18 %. Sodium, magnesium, potassium and iron are less than 10 % of the weight of the sample. After dissolution, carbon percentages of weight increase around 10 % (T: −45, p: 0.008) while weight percentages of calcium (T: 45, p: 0.008) and magnesium (T: 42, p: 0.01) decrease.

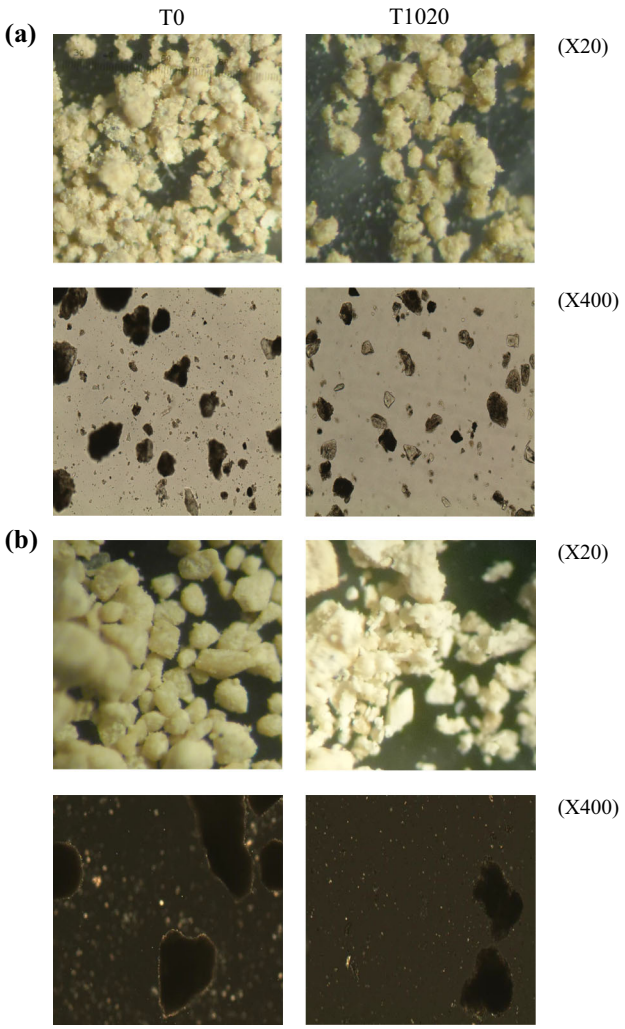

Fig. 8 Photography of loess L1 (**a**) and calcrete C1 (**b**) before (T0) and after 1020 min of reaction (T1020) in batch experiments

Discussion

Physical properties and mineralogical characterization

Pye (1995) describes the "typical" loess as being composed mostly of quartz silt particles and containing more than 50 % of silt size particles, in the size range of 0.002–0.063 mm. In a detailed stratigraphic study in the zone of Mar del Plata (Zárate 1989), the major size component was determined as being fine sand and coarse silt. Regarding to the mineralogical composition, Pye (1995) indicated that loess in Argentina has a high content of feldspar.

From these previous studies, the samples used in this study can be considered representative of the typical loess-like sediments in the area. Results of scanning electron microscopy showed that half of the loess sample is composed of silicon and the other principal components are aluminum and carbon. These results match with the crystallography, as quartz and aluminosilicates principal components are silicon and aluminum. Sodium and calcium are part of the albite and the anorthite feldspars ($NaAlSi_3O_8$, $CaAl_2Si_2O_8$). Magnesium composes the mineral brucite, and titanium composes the mineral anatase. The major elements detected by SEM–EDAX in calcrete are calcium, carbon, silicon and aluminum. The results of this analysis are coherent, as calcite is made of carbon and calcium, quartz is made of silicon and aluminosilicates like albite and anorthite are mostly constituted by silicon and aluminum.

Dissolution experiments

Water analysis

The results of batch experiments indicate that the chemical composition of water experiments differs when loess, calcrete or mix sample dissolve, evolving in dependence of the contact time between sediments and water. An important effect of the particles size is observed specially for C2. In that case, the highest pH values are correlated with the highest concentration of bicarbonate, sulfates, fluoride and an important content of silica is found. Most of the chemical differences observed in the final solutions after each batch essay can be explained by equilibrium reactions, considering 400 min of contact water–sediments. As an example, the lowest calcium content and the lowest rate of calcium incorporation into water are obtained for that sample. The saturation index showed that solution is oversaturated in calcite; this explains why a low concentration of calcium can be released in solution.

In loess, calcium content and incorporation rate are high, particularly in total loess. The calcium must be provided by fast cationic exchange. Bicarbonate content in loess batch reaction is the lowest, and the resulting solution is undersaturated and allows the ion Ca^{2+} incorporating rapidly into water.

Inverse modeling shows that calcite dissolution involves CO_2 incorporation, cation exchange, releasing sodium and uptaking calcium, as well as gypsum dissolution. Those models validate the mass balance of the previous discussion.

High concentration of Na^+ is also obtained when loess is reacting. SEM shows that chlorides move totally to solution after batch experiments. The presence of Na^+ in water must come from the dissolution of NaCl. The dissolution of albite is a very low reaction that cannot be affecting the composition of 400-min essays. Sodium concentration and rate of incorporation are high in impure calcrete; this is probably due to the release of calcium by

Table 1 Rate of ion incorporation in water. *source*: (Martinez and Osterrieth 2013)

	L1		L2		C1		C2		M2		Well P4
	[A]0[a]	r[b]	[A]0	r	[A]0	r	[A]0	r	[A]0	r	[A]0
HCO_3^-	0.55	0.165	0.70	0.180	5.76	0.046	12.15	0.033	5.79	0.439	9.46
Ca^{2+}	3.42	0.855	3.22	0.787	0.30	0.085	0.18	0.006	0.28	0.016	3.34
Na^+	3.58	0.079	3.16	0.029	0.81		0.80	0.043	1.72	0.554	8.26
SiO_2	0.46	0.011	0.70	0.003			1.83	0.014	2.97	0.060	0.98
SO_4^{-2}	0.27	0.002	0.25	0.004	0.17	0.004	2.39	0.184			0.28
K^+	0.14	0.005	0.17	0.002	0.04	0.057	0.12	0.003	0.18	0.005	0.23
F^-	0.09	0.0008	0.07	0.013	0.07	0.001	0.12	0.005	0.10	0.029	0.03

[a] concentrations in mmol/l

[b] rate in mmol/min

Table 2 Netpath inverse models showing the mass balance for the proposed processes in L2, C2 and M2 after 1200 min of sediment–water reaction (values in mmol/L)

Initial solution	Final solution after reacting 1200 min with:	Calcite dissolution	Exchange (Ca^{2+} adsorp., Na^+ release)	Gypsum dissol./precip.
Deionized water	L2	0.851	0.420	0.471
Deionized water	C2	1.741	1.895	0.725
Deionized water	M2	1.776	1.290	−0.004

Table 3 Average oxides percentage of sediments weight (%w) from semi-quantitative analysis of sieved loess, calcrete and mixed sample (L2, C2, M2), before batch experiments (T0) and after 1020 min of reaction

Oxides	L2		C2		M2	
	T0*	T1020*	T0*	T1020*	T0*	T1020*
CO_2	12.5 ± 4.6	8.0 ± 5.2	35.3 ± 3.7	45.7 ± 2.9	28.9 ± 5.8	37.7 ± 4.0
F_2O	0.1 ± 0.3	0.0 ± 0.0	–	–	–	
Na_2O	3.0 ± 1.0	2.1 ± 0.8	0.6 ± 0.4	0.2 ± 0.5	0.4 ± 0.6	0.8 ± 0.9
MgO	2.6 ± 0.7	1.6 ± 0.3	1.6 ± 0.2	1.1 ± 0.4	1.7 ± 0.6	1.2 ± 0.3
Al_2O_3	25.6 ± 4.4	24.3 ± 2.0	8.7 ± 1.3	7.2 ± 3.5	13.3 ± 1.9	13.3 ± 2.6
SiO_2	48.8 ± 5.7	49.3 ± 3.2	16.2 ± 1.4	11.2 ± 4.9	27.2 ± 3.7	25.8 ± 3.3
Cl_2O_3	0.1 ± 0.3	0.0 ± 0.0	0.7 ± 0.4	0.0 ± 0.0	–	–
K_2O	0.8 ± 0.7	2.9 ± 0.5	0.9 ± 0.3	0.3 ± 0.6	1.5 ± 0.2	1.5 ± 0.3
CaO	1.3 ± 0.3	2.6 ± 0.4	33.0 ± 4.4	32.0 ± 4.4	21.1 ± 3.1	15.0 ± 4.3
TiO	2.0 ± 0.7	0.9 ± 0.5	–	–	–	0.7 ± 0.4
MnO	2.6 ± 1.6	0.0 ± 0.0	–	–	–	–
FeO	0.6 ± 0.2	8.3 ± 1.2	2.9 ± 0.5	2.3 ± 0.7	4.6 ± 0.7	4.1 ± 0.7

* Percentage of weight for each sample (%w)

$CaCO_3$ dissolution and its cationic exchange by sodium added to clay particles.

In C2 experiments, a high content of sulfate is observed and the rate of incorporation of this ion in water is particularly high in that case. Sulfur could not be identified in the SEM–EDAX analysis, but gypsum has been found in the Pampeano aquifer (Auge and Hernández 1984) which could be the origin of the ion SO_4^{-2}. In general, gypsum is mixed with calcrete aggregates, which could explain the high concentration of sulfates when dissolving calcrete and could also be a source of calcium incorporation. Sieving calcrete sample must allow the gypsum included in the aggregates to enter in contact with water. Another source of sulfates could be mirabilite ($Na_2SO_4{\cdot}10H_2O$).

Kitano and Okumura (1973) suggest that fluoride precipitate during nucleation of $CaCO_3$. The presence of fluoride in water reacting with calcrete is probably the result of the dissolution of the fluoride precipitated with the calcium carbonates. Furthermore, dissolution of C2 resulted in the highest fluoride content. Previous studies (Turner et al. 2005) showed that the degree of removal of fluoride is directly dependent on the calcite surface area. In the batch

experiment performed in this work, the increasing of surface area by sieving must permit the fluoride to be released more easily in solution.

Batch reaction on L1 and L2 presents a high concentration of fluoride. The origin of this fluoride is supposed to be the dissolution of volcanic ashes in loess (Nicolli et al. 1989; Alarcón-Herrera et al. 2013). The highest concentration of fluoride and rate of incorporation are observed in water dissolving impure calcrete that is composed by the mix of both loess and calcrete. The high pH and the presence of more volcanic ashes must be responsible of the release of fluoride in water for this batch experiment. The origin of fluoride in sediments of the Pampa as released by dissolution of fluorapatite presents either as detritic grains or as forming thin coats onto the volcanic ash has been recently stated (Garcia et al. 2014). García et al. (2012) concluded that biotite weathering is the main source of fluoride in waters in a sector of the center of Argentina, but not dominated by loess sediments.

The highest concentration of silica is obtained when dissolving C2 or M2. With impure calcrete, the concentration of silica and the rate of incorporation of this ion in water are particularly high. This can be explained by the fact that impure calcrete contains more silica and aluminosilicates than pure calcrete. In general, the dissolution of SiO_2 seems to be enhanced in condition of high pH, high bicarbonate content and a small particle size. When dissolving loess or pure calcrete, the concentration of SiO_2 is higher when small particle size reacts. SiO_2 content seems to be dependent on the surface area dissolving.

Some similarities in ion concentration can be found between the results of batch dissolution and groundwater analyses in the sampling zone (Martinez and Osterrieth 2013), but none of the sample allows obtaining the exact proportion and concentrations of the chemical elements than the groundwater sample. The water chemistry of this aquifer must be the result of the dissolution processes of both components at the same time, and a combination of reaction rates. Water dissolving impure calcrete has almost three times more silica than the reference groundwater sample. As observed earlier, small particle size leads to a higher SiO_2 water content. In the aquifer, the sediments are aggregated and this can limit the incorporation of dissolved silica into groundwater.

Oversaturation for calcite in sample of sieved loess, calcrete and mixed sample is reached in the first minutes of reaction. The positive value of SI in these cases must be due to the release of calcium from another source than calcite. Calcium could be released by cationic exchange with Na^+. SiO_2 in water must be provided not only by quartz dissolution but also by the dissolution of amorphous silica minerals, which are very common in the Pampeano sediments.

An important result according to the objectives of the paper is the time elapsed, for each analyzed component, into achieving a constant concentration, i.e., to reach the equilibrium. Most of the variables (pH and dissolved ions) reach the equilibrium concentration after 30–60 min of reaction, but in some cases, more time is necessary depending on the reactive solid phase. The pH and alkalinity demand around 600 min for C1, and alkalinity is continuously increasing for C2 (Fig. 3), which is consequence of the progress of calcite dissolution when major reactive surface is available. Calcium and sodium concentrations become stable after about 120 min, in processes dominated by cationic exchange. The equilibrium in dissolved silica concentrations is not achieved after the 1200 min of batch experiments. This can be expected because of the low solubility of silicates and silica in general and the observed concentration are supposed coming from amorphous silica dissolution, mainly for loess samples.

Sediments analysis

Sediments observation shows that after reacting with water, the smallest particles mainly disappear. Ions in water originate from the dissolution of the smallest dust and aggregates in sediments. Quantitative EDAX analysis also showed significant changes in the proportion of chemical elements constituting the minerals when ions are incorporated into water. Another source of ions in water is the dissolution of coarser sediments particles. Hodson (1998) and Gauthier et al. (2001) showed that decreasing the grain size increases BET surface area and micropore surface area. The increment of surface area is also due to increasing of external surface roughness (White and Brantley 1995). Both loess and calcrete samples BET and micropore surface area increase after batch experiments. In contact with water, the studied sediments dissolve and the chemical components are incorporated into the water.

Conclusion

The kinetics of ions incorporation into water was studied performing batch experiments on loess and calcrete during 10 h. Most of the dissolved ions achieve the equilibrium concentration during the two first hours of reaction, and it takes until 6–8 h for the remaining substance. A more detailed differentiation can be made depending on the type of material, and the particle size in the experiment.

Nevertheless, the individual dissolution of each component of the Pampeano aquifer could not reproduce the exact chemistry of the groundwater in this region. The chemistry of the water is the result of both loess and

calcrete dissolution and their proportion and the size of the particles dissolving. This reaction time needed to get a constant concentration is much shorter than the MRT of groundwater, which is supporting the validity of using equilibrium assumption in most of the study cases of hydrochemistry in the Pampeano aquifer. Silica concentrations can demand more time to reach the equilibrium concentration. The changes observed in the sediments before and after experiment demonstrate an important dissolution process, despite the limited time of the experiment duration.

Going forward, it will be necessary to realize reaction of dissolution with flow-through experiments in order to improve the calculation of the rates of ions incorporation. This technique enables to avoid both the saturation and the reprecipitation bias. The size and the surface area of mineral particles are an important factor for determining the chemistry of water. Changes in micropore and BET surface area were observed in this experience. These variations will be studied in a forthcoming experiment including vertical scanning interferometry in order to determine more accurately rate laws. It will be important to consider every mineral present in the system and their structure when creating models representing geochemical processes like dissolution in natural conditions in the Pampeano aquifer.

Acknowledgments The National Agency for Science and Technology Promotion (ANPCyT, BID-PICT N°0768) supported this study financially. The authors are also thankful to Mr. G. Bernava for chemical analysis, Dr. Mariana Camino for PSD determination, and Dr. Margarita Osterrieth for binocular loupe and petrographic microscopy observations. The authors thank anonymous reviewers for their constructive comments and criticisms.

References

Alarcón-Herrera J, Bundschuh B, Nath HB, Nicolli M, Gutierrez M (2013) Co-occurrence of arsenic and fluoride in groundwater of semi-arid regions in Latin America: genesis, mobility and remediation. J Hazard Mater 262:960–969. doi:10.1016/j.jhazmat.2012.08.005

Ameghino F (1880) La formación Pampeanoa o estudio sobre los terrenos de transporte de la Cuenca delPlata. G Masson, Paris

Auge M, Hernández MA (1984) Características geohidrologicas de un acuífero semiconfinado en la llanura Bonarense. Coloquio Internacional de Grandes llanuras. UNESCO(III). Paris—Buenos Aires

Bocanegra EM (1993) Hydrogeochemical modeling of the process of salinization in Mar del Plata aquifer] Temas Actuales de la Hidrología Subterránea. Publishing Service of the Universidad Nacional De Mar Del Plata, Mar Del Plata, pp 349–360

Bocanegra EM, Benavente M, Cionchi JL (1995) Mathematical simulation of chloride transport in Mar del Plata aquifer. Ser Correlación Geol UN Tucuman 11:25–32

Brady PV, Walther JV (1989) Controls on silicate dissolution rates in neutral and basic pH solutions at 25 °C. Geochim Cosmochim Acta 53:2823–2830. doi:10.1016/0016-7037(89)90160-9

Brady RV, Walther JV (1990) Kinetics of quartz dissolution at low temperatures. Chem Geol 82:253–264. doi:10.1016/0009-2541(90)90084-K

Brantley SL, Kubicki JD, White AF (2008) Kinetics of water-rock interaction, vol 168. Springer, New York. ISBN 978-0-387-73562-7

Cama J, Ganor J, Ayora C, Lasaga CA (2000) Smectite dissolution kinetics at 80°C and pH 8.8. Geochim Cosmochim Acta 64(15):2701–2717. doi:10.1016/S0016-7037(00)00378-1

Chou L, Garrels RM, Wollast R (1989) Comparative study of the kinetics and mechanisms of dissolution of carbonate minerals. Chem Geol 78:269–282. doi:10.1016/0009-2541(89)90063-6

Critelli T, Marini L, Schott J, Mavromatis V, Apollaro C, Rinder T, De Rosa R, Oelkers EH (2014) Dissolution rates of actinolite and chlorite from a whole-rock experimental study of metabasalt dissolution from $2 \leq pH \leq 12$ at 25 C. Chem Geol 390:100–108. doi:10.1016/j.chemgeo.2014.10.013

Critelli T, Marini L, Schott J, Mavromatis V, Apollaro C, Rinder T, Oelkers EH (2015) Dissolution rate of antigorite from a whole-rock experimental study of serpentinite dissolution from $2 < pH < 9$ at 25 C: implications for carbon mitigation via enhanced serpentinite weathering. Appl Geochem 61:259–271. doi:10.1016/j.apgeochem.2015.06.004

Daval D, Hellmann R, Martinez I, Gangloff S, Guyot F (2013) Lizardite serpentine dissolution kinetics as a function of pH and temperature, including effects of elevated pCO2. ChemGeol 351:245–256. doi:10.1016/j.chemgeo.2013.05.020

Dixit S, Carroll SA (2007) Effect of solution saturation state and temperature on diopside dissolution. Geochem Trans 8:3. doi:10.1186/1467-4866-8-3

Dove PM (1999) The dissolution kinetics of quartz in aqueous mixed cation solutions. Geochim Cosmochim Acta 63:3715–3727. doi:10.1016/S0016-7037(99)00218-5

Dove PM, Crerar DA (1990) Kinetics of quartz dissolution in electrolyte solutions using a hydrothermal mixed flow reactor. Geochim Cosmochim Acta 54:955–969. doi:10.1016/0016-7037(90)90431-J

Fagerlund G (1973) Determination of specific surface by the BET method. Mater Struct 6:239–245. doi:10.1016/0016-7037(90)90431-J

Fagundo JR, Valdés JJ, Rodríguez JE (1996) Química del agua kárstica. Hidroquímica del Karst 1:13–212

Fagundo JR, González P, Rodríguez M (2004) Aplicaciones de la cinética en la hidrogeología y el medio ambiente. Contribución a la Educación y la Protección Ambiental, La Habanna

Garcia MG, Borgnino L, Bia G, Depetris P (2014) Mechanisms of arsenic and fluoride release from Chacopampean sediments (Argentina). Int J Environ Health 7(1):41–57. doi:10.1504/IJENVH.2014.060122

García MG, Lecomte KL, Stupar Y, Formica SM, Barrionuevo M, Vesco M, Gallará R, Ponce R (2012) Geochemistry and health aspects of F-rich mountainous stream sand groundwaters from sierras Pampeanas de Cordoba, Argentina. Environ Earth Sci 65:535–545

Garrels RM, Christ CL (1965) Solutions, minerals, and equilibrium. Harper & Row. Harper's geoscience series, New York

Gautier JM, Oelkers EH, Schott J (2001) Are quartz dissolution rates proportional to BET surface areas? Geochim Cosmochim Acta 65(7):1059–1070. doi:10.1016/S0016-7037(00)00570-6

Gomez ML, Martinez DE (2010) Municipal waste management and groundwater contamination processes in Córdoba Province, Argentina. Ambiente Água. Interdiscip J Appl Sci 5:28–46

Herrero AC, Fernández L (2008) De los ríos no me río: diagnóstico y reflexiones sobre las cuencas metropolitanas de Buenos Aires: Luján, Reconquista, Matanza-Riachuelo, de la Ciudad Autónoma de Buenos Aires y de la Zona Sur. Temas Grupo Editorial

Hodson ME (1998) Micropore surface area variation with grain size in unweathered alkali feldspars: implications for surface roughness and dissolution studies. Geochim Cosmochim Acta 62(21):3429–3435. doi:10.1016/S0016-7037(98)00244-0

House WA, Orr DR (1992) Investigation of the pH dependence of the kinetics of quartz dissolution at 25 C. J Chem Soc Faraday Trans 88(2):233–241. doi:10.1039/FT9928800233

Ingram RL (1971) Sieve analysis. In: Carver RE (ed) Procedures in Sedimentary Petrology. Wiley, New York, pp 49–67

Kitano Y, Okumura M (1973) Coprecipitation of fluoride with calcium carbonate. Geochem J 7:37–49. doi:10.2343/geochemj.7.37

Kruse E, Ainchil J (2003) Fluoride variations in groundwater of an area in Buenos Aires Province, Argentina. Environ Geol 44:86–89. doi:10.1007/s00254-002-0702-0

Luce RW, Bartlett WB, Parks GA (1972) Dissolution kinetics of magnesium silicates. Geochimicaet Cosmochimica Acta 36:35–50. doi:10.1016/0016-7037(72)90119-6

Lüttge A (2005) Etch pit coalescence, surface area, and overall mineral dissolution rates. Am Mineral 90:1776–1783. doi:10.2138/am.2005.1734

Martinez DE, Osterrieth MO (2013) Hydrochemistry of an aquifer in Quaternary loess like sediments in the Pampean Plain, Argentina. Revista Facultad de Ingeniería de la Universidad de Antioquia, Colombia 66:9–23 **ISSN 0120-6230**

Martinez DE, Bocanegra ME, Cionchi JL (1995) Modelación hidrogeoquímica de procesos de mezcla. Su aplicación a casos de estudio en el acuífero de Mar del Plata II Seminario Hispano-Argentino Sobre Temas Actuales de la Hidrología Subterránea. Serie Correlación Geológica N 11:69–80

Martinez DE, Massone HE, Ferrante A, Bernava G, Yedaide M (2004) Impacto del lixiviado de rellenos sanitarios en la Cuenca del Arroyo Lobería. Caracterización de la carga contaminante. Revista Latino-Americana de Hidrogeología 457:65

Martinez DE, Fourre E, Quiroz Londoño OM, Jean-Bapiste P, Glok Galli M, Dapoigni A, Grondona S (2015) Residence time distribution in a large unconfined-semiconfined aquifer in the Argentine's Pampas using 3H/3He and CFCs tracers. Hydrogeology Journal, in press

Morse JW (1978) Dissolution kinetics of calcium carbonate in sea water: VI. The near-equilibrium dissolution kinetics of calcium carbonate-rich deep sea sediments. Am J Sci (United States), 278(3)

Morse JW (1983) The kinetics of calcium carbonate dissolution and precipitation. Rev Mineral Geochem 11(1):227–264

Nicolli H, Suriano J, Gomez Peral M, Ferpozzi L (1989) Groundwater Contamination with Arsenic and other trace elements in an area of the Pampa, Province of Córdoba, Argentina. Environ Geol Water Sci 14(1):3–16. doi:10.1007/BF01740581

Paoloni JD, Fiorentino CE, Sequeira ME (2003) Fluoride contamination of aquifers in the southeast subhumid pampa, Argentina. Environ Toxicol 18(5):317–320. doi:10.1002/tox.10131

Parkhurst DL, Appelo CAJ (1999) A computer program for speciation, batch reaction, one dimensional transport and inverse geochemical calculation. U.S. Geological Survey Water-Resources Investigations Report 99-4259

Pokrovsky OS, Schott J (2002) Surface chemistry and dissolution kinetics of divalent metal carbonates. Environ Sci Technol 36:426–432. doi:10.1021/es010925u

Pye K (1995) The nature, origin and accumulation of loess. Quat Sci Rev 14:653–667. doi:10.1016/0277-3791(95)00047-X

Schultz C, Castro E (2003) Estudio planificación y explotación del agua subterránea Una trilogía utópica en la República Argentina. III Congreso Argentino de Hidrogeología. Actas I. Rosario, Argentina, pp 219–225

Smith ME, Knauss KG, Higgins SR (2013) Effects of crystal orientation on the dissolution of calcite by chemical and microscopic analysis. Chem Geol 360:10–21. doi:10.1016/j.chemgeo.2013.09.015

Teruggi ME (1957) The nature and origin of Argentine loess. J Sediment Res 27(3):322–332

Tester JW, Worley WG, Robinson BA, Grigsby CO, Feerer JL (1994) Correlating quartz dissolution kinetics in pure water from 25 - to 625°C. Geochimica et Cosmochimica Acta 54(4):955–969. doi:10.1016/0016-7037(94)90020-5

Tricart J (1973) Geomorfología de la Pampa Deprimida: base para los studios edafológicos y agronómicos; Plan Mapa de Suelos de la Región Pampeana. Secretaría de Estado de Agricultura y Ganadería de la Nación, Inst. Nacional de TecnologíaAgropecuaria INTA

Turner BD, Binning P, Stipp SLS (2005) Fluoride removal by calcite: evidence for fluorite precipitation and surface adsorption. Environ Sci Technol 39:9561–9568. doi:10.1021/es0505090

Van Cappellen P (1996) Reactive surface area control of the dissolution kinetics of biogenic silica in deep-sea sediments. Chem Geol 132:125–130. doi:10.1016/S0009-2541(96)00047-2

Van Cappellen P, Qiu L (1997) Biogenic silica dissolution in sediments of the Southern Ocean. I. Solubility. Deep Sea Res Part II 44(5):1109–1128. doi:10.1016/S0967-0645(96)00113-0

White AF, Brantley SL (1995) Chemical weathering rates of silicate minerals: an overview. Rev in Miner 31:583

Xiao Y, Lasaga AC (1996) Ab initio quantum mechanical studies of the kinetics and mechanisms of Quartz dissolution OH^- catalysis. Geochim Cosmochim Acta 60:2283–2295. doi:10.1016/0016-7037(96)00101-9

Zárate, MA (1989) Estratigrafía y geología del Cenozoico tardío aflorante en los acantilados marinos comprendidos entre Playa San Carlos y el arroyo Chapadmalal, Partido de General Pueyrredón, Provincia de Buenos Aires (Doctoral dissertation, Facultad de Ciencias Naturales y Museo)